www.czasopisma.pan.pl PAN POLSKA AKADEMIA NAUK www.journals.pan.pl

ARCHIVES OF ACOUSTICS Vol. 49, No. 1, pp. 121–128 (2024), doi: 10.24425/aoa.2024.148766

Technical Note

Low-Frequency Sound Absorption Potential of Subwavelength Absorbers Based on Coupled Micro-Slit Panels

Yujie QIAN*, Zhengyuan GAO, Jie ZHANG

College of Information Science and Engineering, Hohai University
Changzhou, China

*Corresponding Author e-mail: 20141923@hhu.edu.cn

(*received February 21, 2023; accepted August 26, 2023; published online December 15, 2023*)

Due to space limitations during installation, reducing low-frequency noise has always been a challenging area. Sub-wavelength structures are typically favored in such scenarios for noise reduction. This paper explores the potential of micro-slit panels (MSP) for low-frequency sound absorption. To further optimize the panel thickness, coupled MSPs (CMSP) with a distance between two MSPs of less than 1 mm are proposed. Firstly, the low-frequency absorption performances of a single MSP based on two optimized schemes – the cavity-depth optimal scheme (COS) and the panel thickness optimal scheme (TOS) – are examined and compared with those of existing ultrathin metamaterials. The results demonstrate that MSP has significant potential for low frequency sound absorption, and COS allows for a smaller overall structural thickness but a larger panel thickness than TOS. Secondly, to reduce the panel thickness, the CMSP is developed and the theoretical model of its acoustic impedance is established and validated by experiments. Then, based on the theoretical model, the low-frequency absorption potential of CMSP is optimized using COS. The results show that both the overall thickness and the panel thickness of the CMSP absorber are reduced while maintaining better performance. Furthermore, the proposed absorber achieves a subwavelength scale since its total thickness can be as small as 0.138λ.

Keywords: coupled MSP (CMSP); cavity-depth optimal scheme (COS); panel thickness optimal scheme (TOS); low frequency; absorption performance.

1. Introduction

The absorption of low-frequency (i.e., 100 to 500 Hz) noise has persistently posed a challenge due to the inherent weak dissipation of classic sound-absorbing materials (MA, SHENG, 2016; ALLARD, ATALLA, 2009). Despite the progress made by active noise reduction approaches in reducing low-frequency noise, the complexity of the devices may prevent from finding their practical use. In practical applications, porous/fibrous materials, resonance-type structures such as micro-perforated panels (MPP) (MAA, 1998; PARK, 2013; WU *et al.*, 2019; XU *et al.*, 2020; LIU *et al.*, 2021a), and micro-slit panels (MSP) (MAA, 2000; RANDEBERG, 2000), are typically preferred. While sound absorbing structures made of porous/fibrous materials are an effective noise absorbing structure, they often require a body thickness comparable to the operating wavelength, which seriously hinders their application in the low-frequency range. Resonance-type structures (MPP and MSP) are regarded as the most promising sound-absorbing materials due to their simple structure, variety of material options and environmental friendliness.

Recently, it has become a balanced goal in low-frequency noise control to reduce the dimension of sound-absorbing structures (i.e., their total thickness) to well below subwavelength. This not only contributes to space savings but also responds to the trend of device miniaturization (CHONG *et al.*, 2010; MEI *et al.*, 2012). Many resonance-type metamaterials targeting low-frequency noise have been studied and developed in this direction, including metamaterial panels based on thin closed slits (JIMÉNEZ *et al.*, 2016; 2017a; 2017b), subwavelength systems with space-coiling structures (LIANG, LI, 2012; CAI *et al.*, 2014; ZHU *et al.*, 2019; ALMEIDA *et al.*, 2021a; WANG *et al.*, 2018; LIU *et al.*, 2021b; WU *et al.*, 2021; SHEN *et al.*, 2019; RYOO, JEON, 2018), a slim

subwavelength absorber (Zhao *et al.*, 2018; Donda *et al.*, 2019; Almeida *et al.*, 2021b), a multicoiled acoustic metasurface (Cheng *et al.*, 2015; Liu *et al.*, 2017) and a micro-perforated panel and coiled-up channel-based hybrid absorber (Li, Assouar, 2016).

The majority of recent research, however, has focused on creating coiled-up space inside cavities in order to extend the acoustic wave's effective propagation distance, thereby allowing for the thinning of absorbing structure in order to absorb low-frequency noise. Studies have shown that when the other structural parameters of MPP or MSP remain the same, the increase in panel thickness causes the sound resonance frequency to shift to lower frequencies. This is because the increase in panel thickness may not only result in an increase in the amount of air mass in the perforation/slit of the panel (i.e., an increase in reactance of the acoustic mass) but also significantly contributes to greater energy dissipation due to greater friction. Consequently, the absorption peak is shifted to lower frequencies (Vigran, 2014). However, the increase in panel thickness will, on one hand, increase the weight of the acoustic structure and, on the other hand, cause an increase in processing costs. Studies have shown that when other structural parameters of MPP or MSP remain the same, an increase in panel thickness causes the sound resonance frequency to shift to lower frequencies. This is because the increase in panel thickness may not only result in an increase in the amount of air mass in the perforation/slit of the panel (i.e., an increase in reactance of the acoustic mass), but also contributes significantly to a greater dissipation of the energy due to the greater friction, and thus shifting the absorption peak to lower frequencies (Vigran, 2014). But an increase in panel thickness will, on one hand, increase the weight of the acoustic structure and, on the other hand, cause an increase in processing costs.

It is widely recognized that the acoustic impedance of the micro-slits is proportional to the panel thickness (Maa, 2000; Randeberg, 2000). And vice versa, an increase in acoustic impedance corresponds to an increase in effective panel thickness. Based on this, this paper proposes a coupled MSPs, which consists of two MSPs with a distance of less than 1 mm between them, forming inter-panel micro-slits. As a result, the acoustic impedance of this proposed structure is not only provided by the micro-slits on the panels but also by the micro-slits between the panels. In this way, the equivalent panel thickness can be increased by adjusting the acoustic impedance provided by the micro-slits formed between the panels. Consequently, this approach can be utilized to improve low-frequency sound absorption performance.

The remainder of this paper is organized as follows. The mathematical expression of the normal absorption coefficient and an analytical model of the acoustic impedance for a single MSP absorber are provided in Sec. 2. Based on this, the exhaustive method is used to investigate the minimum cavity depth and the minimum panel thickness required for an MSP absorber at a given resonant frequency and maximum absorption coefficient. Next, the results obtained are then compared with those in existing literature for metamaterials. In Sec. 3, the coupled MSP absorber is proposed and its theoretical model of impedance is developed and validated by experiments. The coupled MSP structure is then used to further optimize the panel thickness, resulting in the reduction of the acoustic structure's total thickness. Finally, the conclusions are drawn in Sec. 4.

2. MSP absorber and its low-frequency absorption performance

2.1. MSP absorber

The basic structure of a traditional MSP absorber consists of a micro-slit panel, a rigid backing wall and the air cavity between them. This is illustrated in Fig. 1a, where d is the slit width, t is the panel thickness, b is the distance between centers of adjacent slits, and D is the depth of the air cavity. Based on the acoustoelectric analogy, the equivalent circuit of an MSP absorber is depicted in Fig. 1b. Here, Z_{MSP} is the specific acoustic impedance of the MSP and Z_D is the specific acoustic impedance of the air cavity. The sound wave impinging on the structure is equivalent to a source of sound pressure $2p$, as produced on the rigid wall with the time factor $\exp(-j\omega t)$ suppressed throughout (analogous to the open-circuit voltage) and internal resistance $\rho_0 c$ as that of air, where ρ_0 is the air density and c is the sound speed in air. The acoustic impedance of a micro-slit with end correction can be given as (Maa, 2000; Randeberg, 2000):

$$Z_{\mathrm{MSP}} = \frac{12\eta t}{d^2}\sqrt{1+\frac{k^2}{18}} + i\rho_0\omega t\left(1+\frac{1}{\sqrt{25+2k^2}}\right)+R_s+iX_m \quad (1)$$

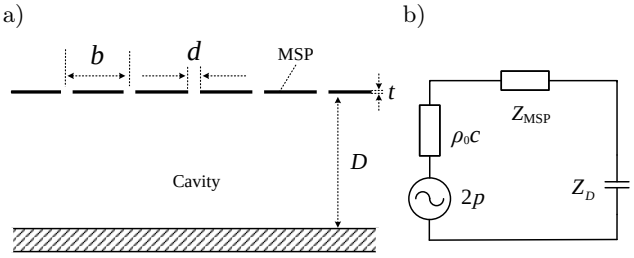

Fig. 1. Schematic diagrams of the composite sound absorber structure and its equivalent circuit.

with

$$k = d\sqrt{\rho_0\omega/\eta}/2, \tag{2}$$

$$R_s = \frac{\sqrt{2\eta\omega\rho_0}}{\sigma}, \tag{3}$$

$$X_m = -\frac{2}{\pi\sigma}\rho_0\omega d\ln\left[\sin\left(\frac{\sigma\pi}{2}\right)\right], \tag{4}$$

where $\omega = 2\pi f$ is the angular frequency with f being the frequency of the incident acoustic wave, σ is the perforation rate of the panel (the ratio of surface area of the slits to the total surface area of the panel), $\sigma = d/b$, i is an imaginary unit, R_s is the resistance end correction, and X_m is the reactance end correction.

The acoustic impedance of the air cavity behind the MPP with a depth of D is given by:

$$Z_D = -j\rho_0 c\cot(\omega D/c). \tag{5}$$

The overall acoustic impedance of an MSP absorber is given by:

$$Z = Z_{\mathrm{MSP}} + Z_D. \tag{6}$$

The normal sound absorption coefficient is calculated using the equation:

$$\alpha = 1 - \left|\frac{Z - \rho_0 c}{Z + \rho_0 c}\right|^2. \tag{7}$$

2.2. Design optimization via exhaustive search

Due to the continuous improvement of computer computing power, the structural parameters of the MSP absorber can be globally designed and optimized by the exhaustive search (Lara-Valencia *et al.*, 2020; Pierro *et al.*, 2021), according to the noise reduction performance requirements. In this study, two parameters related to the sound absorption performance requirements are considered: the resonant frequency f_r and its corresponding absorption coefficient a_r. Once sound absorption requirements are given, an exhaustive search is used to select the combination of structural parameters that meet these requirements. If there are multiple sets of structural parameters that meet the requirements, the unique combination of parameters is determined by two selection schemes: one is to select the one with the smallest depth, smallest panel thickness and the largest resonance absorption coefficient in order of preference, i.e., the cavity-depth optimal scheme (COS), and the other is to give preference to the set with the smallest panel thickness, smallest depth, and the largest resonance absorption coefficient, i.e., the panel thickness optimal scheme (TOS). The combination of structural parameters used for optimization is: the micro-slit width d, panel thickness t, center distance between two adjacent slits b, and cavity depth D. The parameter range for the exhaustive search is:

$$\begin{aligned} &0.1\ \mathrm{mm} \le d \le 1\ \mathrm{mm}; \qquad 0.1\ \mathrm{mm} \le t \le 10\ \mathrm{mm};\\ &0.3\ \mathrm{mm} \le b \le 170\ \mathrm{mm}; \qquad 5\ \mathrm{mm} \le D \le 30\ \mathrm{mm}. \end{aligned} \tag{8}$$

It should be noted that, firstly, the upper limit of the panel thickness is set to less than 10 mm, since the excessive panel thickness will increase the weight and manufacturing cost of the MSP. Secondly, the upper limit for the distance between the centers of adjacent micro-slits is set to 170 mm. This is because the low-frequency range studied in this paper is 100~500 Hz. To ensure the applicability of the above derived analytical equation for the acoustic impedance of the MSP (considering the micro-slits as parallel), the distance between two adjacent micro-slits should be less than 1/4 of the wavelength corresponding to the maximum frequency (Liu *et al.*, 2021).

Moreover, the lower and upper limits of the cavity depth are set to 5 and 30 mm, respectively. This is because, on one hand, this study is dedicated to finding structural parameters that not only meet the sound absorption requirements but also minimize the total thickness, so the upper limit should not be set too large, and, on the other hand, according to previous design experience, the cavity depth is too small to find a suitable combination of structural parameters, so the lower limit of the cavity depth should not be too small either. The search steps for each parameter are 0.01 mm for d and 0.1 mm for t, b, and D, respectively. Furthermore, combinations of parameters where the micro-slit width d is less than the micro-slit spacing b will be discarded.

2.3. Low-frequency absorption potential

Assuming that resonant frequencies studied are 254, 338.5, and 391 Hz, the optimal combination of parameters for different absorption coefficient requirements is determined via exhaustive search based on the specified above selection rules. The results are shown in Table 1, where T indicates the total thickness of the absorber. Note that all length-related variables in the tables of this paper are in millimeters. As can be seen in Table 1, as the required resonant frequency increases, both the required minimum cavity depth and minimum panel thickness decrease accordingly. This is reasonable, because the smaller the frequency the larger the wavelength, and thus the size of the required absorber increases.

Table 1. Performance requirements and the optimal parameter combination for MSP absorbers.

f_r	a_r	Group	D	t	d	b	T
254	≥ 0.98	MSP1-COS	21.7	8.4	0.99	169.8	30.1
		MSP1-TOS	30	3.7	0.73	170	33.7
338.5	≥ 0.98	MSP2-COS	13.4	7.5	0.99	170	20.9
		MSP2-TOS	29.3	0.5	0.38	170	29.8
391	≥ 0.98	MSP3-COS	10.5	7.1	0.99	170	17.6
		MSP3-TOS	25.8	0.1	0.24	170	25.9

To examine the low-frequency sound absorption potential of the MSP with the limited cavity depth, its

absorption coefficients, based on Eq. (7), are compared with those of ultra-thin metamaterials (with the same theoretical resonant frequency) from existing literature (Jiménez *et al.*, 2016; Cai *et al.*, 2014). The schemes of the metamaterials used for comparison are shown in Fig. 2, and their relevant parameters are shown in Table 2. The comparison of the theoretical results for the normal absorption coefficient is presented in Fig. 3.

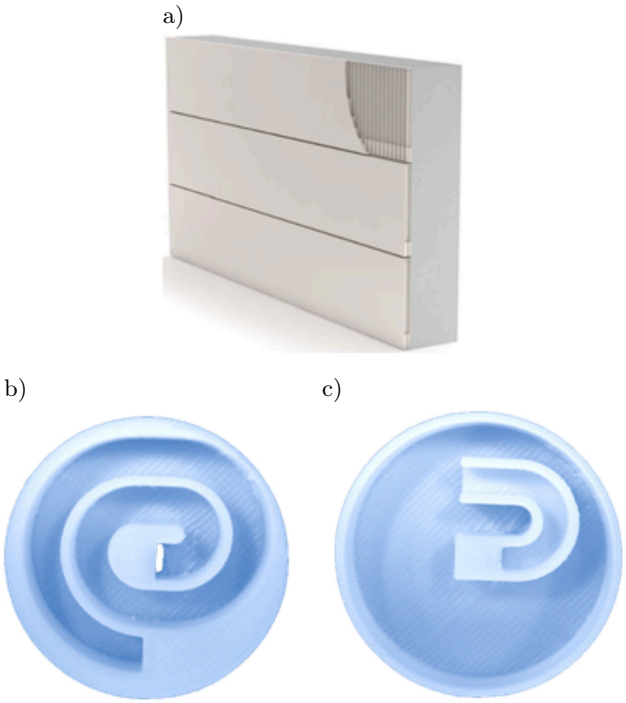

Fig. 2. Schemes of the ultra-thin metamaterial in existing literature: (a) Helmholtz resonator arrays (Jiménez *et al.*, 2016), circular absorbers with embedded (b) coplanar spiral tube, and (c) coplanar resonant chamber (Cai *et al.*, 2014).

Combining the data from Table 1, Table 2, and Fig. 3, several findings can be derived:

a) MSPs have the ability to achieve a maximum absorption value comparable to that of ultrathin metamaterials while maintaining a wider absorption bandwidth. Additionally, the panel-thickness optimal scheme-based MSP absorbers perform even better than the cavity-depth optimal scheme-based MSP absorbers in terms of sound absorption bandwidth. This is attributed to the fact that the bandwidth is proportional to the ratio of acoustic resistance to acoustic mass $\frac{\text{real}(Z_{\text{MSP}})}{\text{imag}(Z_{\text{MSP}})}$, in which real (Z_{MSP}) denotes the real part of the acoustic impedance of the MSP, i.e., acoustic resistance, and imag (Z_{MSP}) represents the imaginary part, i.e., acoustic mass. According to Table 1, the panel thickness optimal scheme-based MSP has a smaller panel thickness and slit width, resulting in a higher ratio of acoustic resistance to acoustic mass, thus yielding a better bandwidth (Maa, 2000; Randeberg, 2000).

b) At the resonant frequency f_r = 391 Hz, the total thickness of the MSP3-COS is almost equal to that of the metamaterial. In other conditions, the total thickness of the MSP absorber is about 1.5 to 2.7 times that of the metamaterial. Meanwhile, the total thickness of the panel thickness optimal scheme-based MSP absorbers is greater than that of the cavity-depth optimal scheme-based MSP absorbers.

c) For cavity-depth optimal scheme-based MSP absorbers, in addition to the cavity depth, the panel thickness significantly contributes to the overall thickness of the absorber.

Table 2. Performance and structural parameters of the ultrathin metamaterials.

Members	Metamaterial	f_r [Hz]	a_r	T
Meta-1	Circular absorber with embedded coplanar resonant chamber (Cai *et al.*, 2014)	254	≥ 0.98	13.3
Meta-2	Helmholtz resonator arrays (Jiménez *et al.*, 2016)	338.5	≥ 0.98	11
Meta-3	Circular absorber with embedded coplanar spiral tube (Cai *et al.*, 2014)	391	≥ 0.97	17

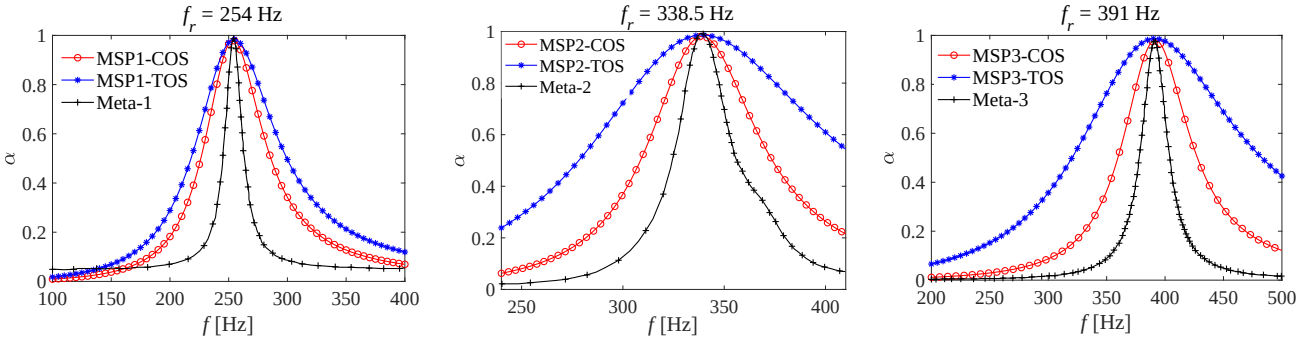

Fig. 3. Comparison of the theoretical normal absorption coefficients between MSP and ultra-thin metamaterials in existing literature.

From the above conclusions, it can be concluded that MSP absorbers exhibit great potential for low-frequency sound absorption in both maximum absorption coefficient and absorption bandwidth. Specifically, the cavity-depth optimal scheme-based MSP absorbers show promise in achieving a balance between better sound absorption performance and a smaller total structure thickness. But, their comparatively larger panel thickness may contribute to an increase in manufacturing cost and structure weight.

3. Optimized panel thickness by using coupled micro-slit panels (CMSP)

3.1. CMSP absorber and theoretical model of its acoustic impedance

In order to further optimize the panel thickness, an absorber based on CMSP is proposed. The CMSP absorber consists of two MSPs with a distance between them being less than 1 mm, fixed before a solid surface with a cavity of depth D, as depicted in Fig. 4a. Here, d_g represents the gap thickness. The micro-slits on the top and bottom panels need to be staggered so that the airflow from the micro-slits of the top panel flows equally into the two adjacent micro-slits of the bottom panel. As shown in Fig. 4b, the micro air gap between MSP1 and MSP2 increases the length of the airflow path, thus can be equivalently regarded as increasing the thickness of the panel. Based on the acoustic-electric analogy, the equivalent circuit of the CMSP can be derived, as shown in Fig. 4c, where the MSP1 is coupled with MSP2 through the acoustic impedance of the micro-slits between the two panels.

It can be seen in Fig. 4b that the role of the air gap between two MSPs is the same as that of the MSP1 and MSP2. Based on the equivalent circuit, the total acoustic impedance of the entire structure can be expressed as

$$Z_{\mathrm{CMSP}} = Z_{\mathrm{MSP1}} + Z_{\mathrm{MSP1\_2}}/2 + Z_{\mathrm{MSP2}}, \qquad (9)$$

where Z_{MSP1}, $Z_{\mathrm{MSP1\_2}}$ and Z_{MSP2} represents the acoustic impedance of MSP1, micro-slits between two MSPs, and MSP2, respectively. It is important to note that the micro-slit width, micro-slit thickness and micro-slit rate of the micro-slits between two MSPs are d_g, $b/2 - d$, and d_g/b, respectively. When the parameters of MSP1 and MSP2 are determined, the acoustic impedance of the CMSP can therefore be adjusted by the micro-slit width d_g alone. The normal sound absorption coefficient can also be calculated according to Eq. (7).

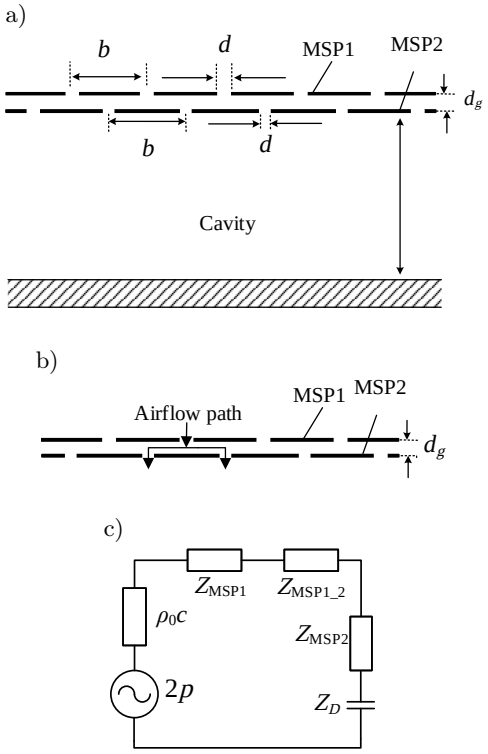

Fig. 4. Schematic diagrams of the CMSP structure and its equivalent circuit.

3.2. Experimental validation

In this section, the experiment is conducted to verify the theoretical results of CMSP. An impedance tube with diameter of 10 cm is used for experimental test, as shown in Fig. 5, with a working frequency range of 90~1800 Hz. The measured frequencies are 1/3 octave center frequencies from 100 to 1600 Hz. The test sample is made from epoxy resign. In order to form a CMSP absorber, a special design of the experimental sample is required in the design phase, and the design diagrams of the top MSP and bottom MSP are shown

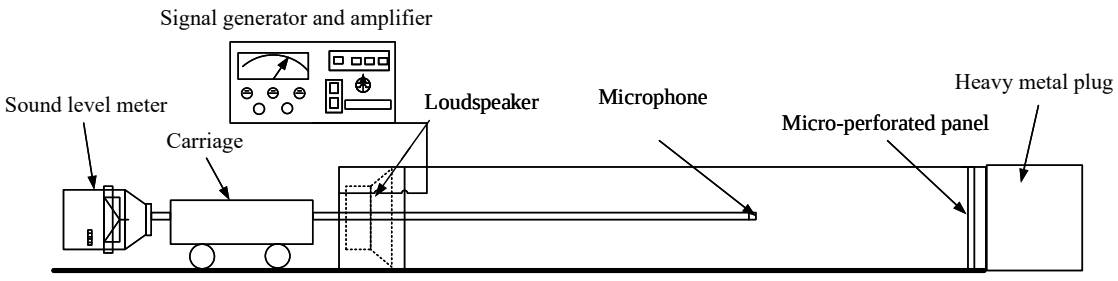

Fig. 5. Layout of the impedance tube.

in Fig. 6. The structural parameters of the samples are shown in Table 3, where the subscripts 1 and 2 denote MSP1 and MSP2, respectively. The experimental samples of CMSP#3 are presented in Fig. 7. The comparison between experiments and theoretical results is depicted in Fig. 8. It is evident from Fig. 8 that the theoretical prediction agrees well with the experimental data, which proves that the theoretical model is reliable.

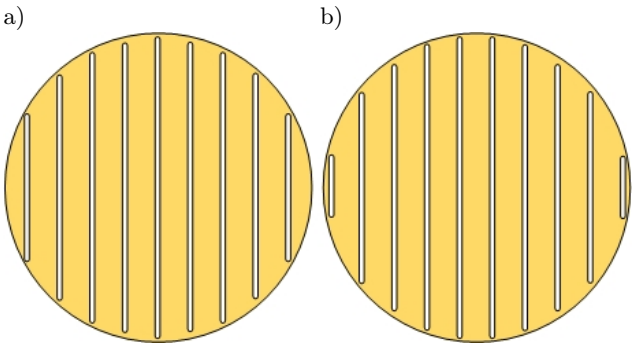

Fig. 6. Design schematic of MSPs: a) top MSP1; b) bottom MSP2.

Table 3. Structure parameters of CMSP absorbers for experiments.

Member	D	$t_{1,2}$	$d_{1,2}$	d_g	b
#1	30	1	0.3	0.2	6
#2	30	1.5	0.5	0.2	8
#3	30	1	0.6	0.3	8
#4	30	1.5	0.6	0.3	9

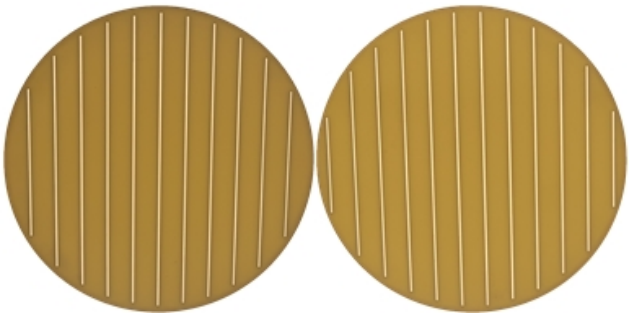

Fig. 7. Experimental samples of CMSP#3 for comparison.

3.3. Panel thickness optimization

The parameter range for the exhaustive search for the CMSP absorber is defined as:

$$\begin{gathered} 0.1 \text{ mm} \le d \le 1 \text{ mm}; \quad 0.1 \text{ mm} \le t \le 1 \text{ mm}; \\ 0.3 \text{ mm} \le b \le 170 \text{ mm}; \quad 0.1 \text{ mm} \le d_g \le 1 \text{ mm}; \\ 5 \text{ mm} \le D \le 30 \text{ mm}. \end{gathered} \tag{10}$$

The selection of the optimal combination of parameters for a CMSP absorber follows the cavity depth optimal scheme (COS). The optimal combinations of parameters selected for the CMSP absorber are shown in Table 4. It shows that the optimal panel thickness can be reduced significantly by the CMSP, with the panel thickness reaching the lower limit of the parameter range as thin as 0.1 mm. Although a panel thickness of 0.1 mm may be impractical in practical applications, it foreshadows the great potential of

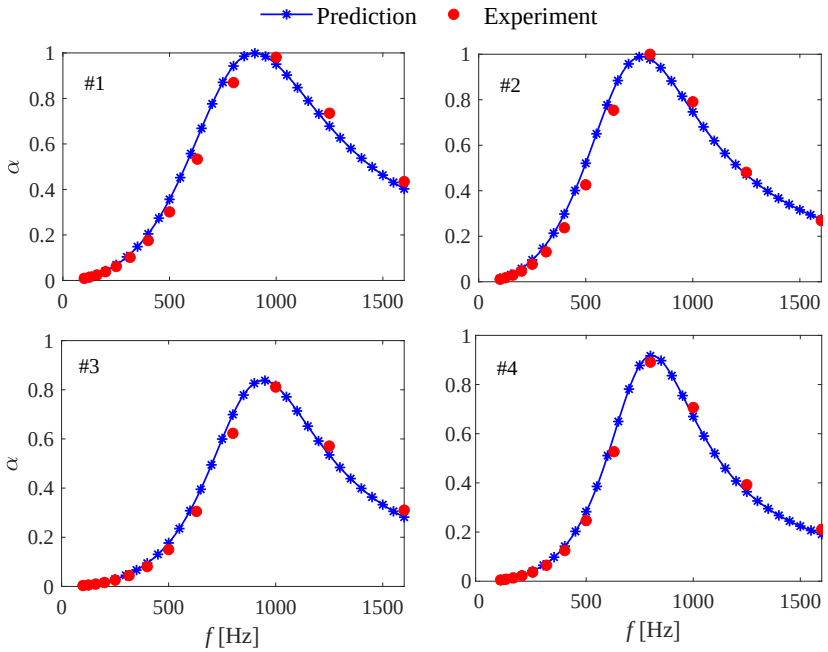

Fig. 8. Comparison between experimental data and theoretical prediction of normal sound absorption coefficient for CMSP absorbers.

Table 4. Theoretically optimal combination of parameters for CMSP absorbers.

Member	f_r	a_r	D	$t_{1,2}$	$d_{1,2}$	d_g	$b_{1,2}$	T
CMSP1	254	≥ 0.98	24.1	0.1	0.94	0.99	77	25.29
CMSP2	338.5	≥ 0.98	15.1	0.1	0.83	0.99	73	16.29
CMSP3	391	≥ 0.98	12	0.1	0.81	0.99	71	12.19

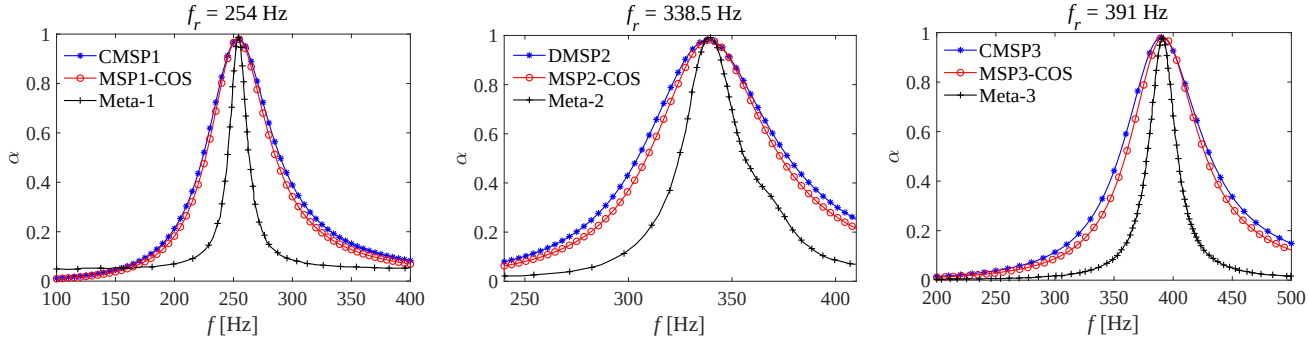

Fig. 9. Comparison of normal absorption coefficients between CMSP, MSP, and ultra-thin metamaterials.

CMSPs in reducing the panel thickness. In practical applications, the structural parameter range for optimization can be flexibly modified based on actual processing conditions. The comparison results of normal absorption coefficients between CMSP absorbers, COS-based MSP absorbers and metamaterials are illustrated in Fig. 9. As can be seen in Table 4 and Fig. 9, for different resonance frequency requirements (254, 338.5, and 391 Hz), although the overall thickness of CMSP absorbers decreases by 16, 22, and 27%, and the panel thickness is reduced by 98.8, 98.6, and 98.5%, respectively, compared to single MSP-COS absorbers, CMSP absorbers still outperform both MSP-COS absorbers and metamaterials in terms of sound absorption bandwidth. In particular, at f_r = 391 Hz, the CMSP achieves better sound absorption performance with less total thickness compared to Meta-3. Moreover, at resonant frequencies of 254, 338.5, and 391 Hz, the total thickness of the CSMPs is 0.187, 0.16, and 0.138 times the resonant wavelength, respectively, demonstarting sub-wavelength dimensions.

4. Conclusion

A subwavelength absorber based on CMSP is proposed and investigated to achieve high absorption in the low-frequency range at a smaller thickness. Firstly, COS and TOS, respectively, are employed to maximize the low-frequency absorption potential of a MSP), demonstrating that COS enables MSP to achieve a smaller total thickness but a higher panel thickness. The CSMPs' acoustic impedance theoretical model is subsequently developed and experimentally verified. Based on the theoretical model, COS is used to optimize the CSMP's low-frequency absorption capability in order to further reduce panel thickness. It is shown that the CSMPs can significantly reduce the panel thickness while maintaining relatively better sound absorption properties compared to both MSP and metamaterials in existing literature. Notably, at a resonance frequency of 391 Hz, the total thickness of the CMSP can reach subwavelength dimension of 0.138λ (λ denotes the resonance wavelength).

Acknowledgments

This work was supported by Aviation Science Foundation (No. 2023Z074108001).

References

1. Allard J.F., Atalla N. (2009), *Propagation of Sound in Porous Media: Modelling Sound Absorbing Materials*, Wiley, Chichester, doi: 10.1002/9780470747339.
2. Almeida G.N., Erasmo F.V., Barbosa L.R., Lenzi A., Birch R.S. (2021a), Sound absorption metasurface with symmetrical coiled spaces and micro slit of variable depth, *Applied Acoustics*, **183**: 108312, doi: 10.1016/j.apacoust.2021.108312.
3. Almeida G.N., Vergara E.F., Barbosa L.R., Brum R. (2021b), Low-frequency sound absorption of a metamaterial with symmetrical-coiled-up spaces, *Applied Acoustics*, **172**: 107593, doi: 10.1016/j.apacoust.2020.107593.
4. Cai X.B., Guo Q.Q., Hu G.K., Yang J. (2014), Ultrathin low-frequency sound absorbing panels based on coplanar spiral tubes or coplanar Helmholtz resonator, *Applied Physics Letters*, **105**: 121901, doi: 10.1063/1.4895617.
5. Cheng Y., Zhou C., Yuan B.G., Wu D.J., Wei Q., Liu X.J. (2015), Ultra-sparse metasurface for high reflection of low-frequency sound based on artificial Mie resonances, *Nature Mater*, **14**: 1013–1019, doi: 10.1038/nmat4393.
6. Chong Y., Ge L., Cao H., Stone A.D. (2010), Coherent perfect absorbers: Time-reversed lasers, *Physi-*

cal Review Letters, **105**(5): 053901, doi: 10.1103/PhysRevLett.105.053901.

7. Donda K., Zhu Y., Fan S.-W., Cao L., Li Y., Assouar B. (2019), Extreme low-frequency ultrathin acoustic absorbing metasurface, *Applied Physics Letter*, **115**(17): 173506, doi: 10.1063/1.5122704.
8. Jiménez N., Romero-García V., Pagneux V., Groby J.-P. (2017a), Quasi-perfect absorption by subwavelength acoustic panels in transmission using accumulation of resonances due to slow sound, *Physical Review Journals*, **957**: 014205, doi: 10.1103/PhysRevB.95.014205.
9. Jiménez N., Romero-García V., Pagneux V., Groby J.-P. (2017b), Rainbow-trapping absorbers: Broadband, perfect and asymmetric sound absorption by subwavelength panels for transmission problems, *Scientific Reports*, **7**: 13595, doi: 10.1038/s41598-017-13706-4.
10. Jiménez N., Huang W., Romero-García V., Pagneux V., Groby J.-P. (2016), Ultra-thin metamaterial for perfect and quasi-omnidirectional sound absorption, *Applied Physics Letters*, **109**: 121902, doi: 10.1063/1.4962328.
11. Lara-Valencia L.A., Farbiarz-Farbiarz Y., Valencia-González Y. (2020), Design of a tuned mass damper inerter (TMDI) based on an exhaustive search optimization for structural control of buildings under seismic excitations, *Shock and Vibration*, **2020**: 8875268, doi: 10.1155/2020/8875268.
12. Li Y., Assouar B.M. (2016), Acoustic metasurface-based perfect absorber with deep subwavelength thickness, *Applied Physics Letter*, **108**(6): 063502, doi: 10.1063/1.4941338.
13. Liang Z.X., Li J. (2012), Extreme acoustic metamaterial by coiling up space, *Physical Review Journals*, **108**: 114301, doi: 10.1103/PhysRevLett.108.114301.
14. Liu C.M., Xia B.Z., Yu D.J. (2017), The spiral-labyrinthine acoustic metamaterial by coiling up space, *Physics Letters A*, **381**(36): 3112–3118, doi: 10.1016/j.physleta.2017.07.041.
15. Liu X., Wang C.Q., Zhang Y.M., Huang L.X. (2021a), Investigation of broadband sound absorption of smart micro-perforated panel (MPP) absorber, *International Journal of Mechanical Sciences*, **199**: 106426, doi: 10.1016/j.ijmecsci.2021.106426.
16. Liu Y.Y., Ren S.W., Sun W., Lei Y., Wang H.T., Zeng X.Y. (2021b), Broadband low-frequency sound absorbing metastructures based on impedance matching coiled-up cavity, *Applied Physics Letter*, **119**(10): 101901, doi: 10.1063/5.0061012.
17. Ma G., Sheng P. (2016), Acoustic metamaterials: From local resonances to broad horizons, *Science Advances*, **2**(2): e1501595, doi: 10.1126/sciadv.1501595.
18. Maa D.Y. (1998), Potential of microperforated panel absorber, *The Journal of the Acoustical Society of America*, **104**(5): 2861–2866, doi: 10.1121/1.423870.
19. Maa D.Y. (2000), Theory of microslit absorbers [in Chinese], *Acta Acustica*, **25**(6): 481–485, doi: 10.15949/j.cnki.0371-0025.2000.06.001.
20. Mei J., Ma G., Yang M. (2012), Dark acoustic metamaterials as super absorbers for low-frequency sound, *Nature Communications*, **3**: 756, doi: 10.1038/ncomms1758.
21. Park S.H. (2013), Acoustic properties of micro-perforated panel absorbers backed by Helmholtz resonators for the improvement of low-frequency sound absorption, *Journal of Sound and Vibration*, **332**(20): 4895–4911, doi: 10.1016/j.jsv.2013.04.029.
22. Pierro V. *et al.* (2021), Ternary quarter wavelength coatings for gravitational wave detector mirrors: Design optimization via exhaustive search, *Physics Review Research*, **3**(2): 023172, doi: 10.1103/PhysRevResearch.3.023172.
23. Randeberg R.T. (2000), *Perforated panel absorbers with viscous energy dissipation enhanced by orifice design*, Ph.D. Thesis, Norwegian University of Science and Technology, Trondheim.
24. Ryoo H., Jeon W. (2018), Perfect sound absorption of ultra-thin metasurface based on hybrid resonance and space-coiling, *Applied Physics Letter*, **113**(12): 121903, doi: 10.1063/1.5049696.
25. Shen Y., Yang Y., Guo X., Shen Y., Zhang D. (2019), Low-frequency anechoic metasurface based on coiled channel of gradient cross-section, *Applied Physics Letter*, **114**(8): 083501, doi: 10.1063/1.5081926.
26. Vigran T.E. (2014), The acoustic properties of panels with rectangular apertures, *The Journal of the Acoustical Society of America*, **135**(5): 2777–2784, doi: 10.1121/1.4871363.
27. Wang Y., Zhao H.G., Yang H.B., Zhong J., Zhao D., Lu Z.L., Wen J.H. (2018), A tunable sound-absorbing metamaterial based on coiled-up space, *Journal of Applied Physics*, **123**(18): 185109, doi: 10.1063/1.5026022.
28. Wu F., Xiao Y., Yu D.L., Zhao H.G., Wang Y., Wen J.H. (2019), Low-frequency sound absorption of hybrid absorber based on micro-perforated panel and coiled-up channels, *Applied Physics Letters*, **114**: 151901, doi: 10.1063/1.5090355.
29. Wu Y., Liang Q., He J., Feng J., Chen T. (2021), Deep-subwavelength broadband sound absorbing metasurface based on the update finger coiling-up method, *Applied Acoustics*, **195**: 108846, doi: 10.1016/j.apacoust.2022.108846.
30. Xu Z.M., He W., Peng X.G., Xin F.X., Lu T.J. (2020), Sound absorption theory for micro-perforated panel with petal-shaped perforations, *The Journal of the Acoustical Society of America*, **148**(18): 18–24, doi: 10.1121/10.0001462.
31. Zhao H., Wang Y., Wen J., Lam Y.W., Umnova O. (2018), A slim subwavelength absorber based on coupled microslits, *Applied Acoustics*, **142**: 11–17, doi: 10.1016/j.apacoust.2018.08.004.
32. Zhu Y.F., Donda K., Fan S.W., Cao L.Y., Assouar B. (2019), Broadband ultra-thin acoustic metasurface absorber with coiled structure, *Applied Physics Express*, **12**: 114002, doi: 10.7567/1882-0786/ab494a.